American Journal of Pathology, Vol. 164, No. 4, April 2004

Interferon-γ-Induced Nitric Oxide Causes Intrinsic Intestinal Denervation in *Trypanosoma cruzi*-Infected Mice

Rosa M.E. Arantes,* Homero H.F. Marche,† Maria T. Bahia,‡ Fernando Q. Cunha,§ Marcos A. Rossi,¶ and João S. Silva†

From the Department of Pathology, Biological Sciences Institute, Federal University of Minas Gerais, Belo Horizonte; the Departments of Biochemistry and Immunology,† Pharmacology,§ and Pathology,¶ Faculty of Medicine of Ribeirão Preto, University of São Paulo, Ribeirão Preto; and the Department of Biological Sciences,‡ Biological Sciences Institute, Federal University of Ouro Preto, Ouro Preto, Brazil*

In this study, the role of nitric oxide (NO) in neuronal destruction during acute-phase *Trypanosoma cruzi* infection was evaluated in male C57BL/6 (WT, wild-type) mice and knockout mice [inducible nitric oxide synthase (iNOS)$^{-/-}$ and interferon (IFN)$^{-/-}$]. Selected animals were infected by intraperitoneal injection of 100 trypomastigote forms of the Y strain of *T. cruzi*. Others were injected intraperitoneally with an equal volume of saline solution and served as controls. Our findings support those of previous studies regarding myenteric denervation in acute-phase *T. cruzi* infection. In addition, we clearly demonstrate that, despite the fact that parasite nests and similar inflammatory infiltrate in the intestinal wall were more pronounced in infected iNOS$^{-/-}$ mice than in infected WT mice, the former presented no reduction in myenteric plexus neuron numbers. Neuronal nerve profile expression, as revealed by the general nerve marker PGP 9.5, was preserved in all knockout animals. Infected IFN$^{-/-}$ mice suffered no significant neuronal loss and there was no inflammatory infiltrate in the intestinal wall. On days 5 and 10 after infection, iNOS activity was greater in infected WT mice than in controls, whereas iNOS activity in infected knockout mice remained unchanged. These findings clearly demonstrate that neuronal damage does not occur in NO-impaired infected knockout mice, regardless of whether inflammatory infiltrate is present (iNOS$^{-/-}$) or absent (IFN$^{-/-}$). In conclusion, our observations strongly indicate that myenteric denervation in acute-phase *T. cruzi* infection is because of IFN-γ-elicited NO production resulting from iNOS activation in the inflammatory foci along the intestinal wall. *(Am J Pathol 2004, 164:1361–1368)*

Chagas' disease, resulting from infection with the protozoan *Trypanosoma cruzi*, is a significant cause of morbidity and mortality in Latin America.[1] Infection with *T. cruzi* includes an acute septicemic phase, during which the parasite infects a wide variety of tissues, mainly muscular tissue and central nervous system. In most patients, specific host defense mechanisms develop within 1 month and the septicemic phase subsides, without any serious sequelae. The acute phase passes into a chronic phase, in which a few parasites remain in the circulating blood and body tissues. Most patients are asymptomatic in the chronic phase of the disease, presenting the so-called indeterminate or latent form, although some patients develop manifestations 10 to 30 years after the onset of infection.[2] These late manifestations typically present as cardiac arrhythmias, cardiomyopathy, or disturbances in esophageal and colonic motility.[3] The final stage of the altered motility involves hypertrophy and dilatation of the organ, ie, megaesophagus and megacolon, particularly the sigmoid colon. The underlying anatomical abnormality in these patients is reduced ganglion cell numbers in the myenteric plexuses. This reduction, assumed to occur in the acute phase of the infection, has been extensively demonstrated through quantitative and comparative studies.[3,4–12]

Although there is currently no consensus, various neuronal destruction mechanisms have been proposed. The presence of a neurotoxic or neurolytic agent, liberated by the disintegrated amastigote forms, has been postulated.[13] It has also been suggested that ganglion cell parasitism could induce direct destruction of the nerve cells.[14] Another hypothesis is that nerve cell degeneration and destruction is related to an immunoinflammatory reaction triggered by the parasites or their antigens in the muscle tissue around the neuronal ganglia.[15–20] More recently, the authors of a study involving *T. cruzi*-infected rats suggested a relationship between nitric oxide (NO) production and ganglion cell loss.[21] An increased ex-

Supported by grants from Fundação du Amparo á Pesquisa de Estado de São Paulo, Fundação du Amparo á Pesquisa de Estado de Minas Gerais, Conselho Nacional de Desenvolvimento Científico e Tecnológico, and DNDP/World Bank/World Health Organization Special Program for Research and Training in Tropical Diseases (grant TDR 990945).

Accepted for publication December 29, 2003.

Address reprint requests to Marcos A. Rossi, M.D., Ph.D., Department of Pathology, Faculty of Medicine of Ribeirão Preto, University of São Paulo, 14049-900, Ribeirão Preto, SP, Brazil. E-mail: marossi@fmrp.usp.br.

pression of nicotine adenine dinucleotide phosphate-diaphorase (NADPH-diaphorase) reaction, an indicator of the cellular localization of NO synthase, in the colon muscle layers of *T. cruzi*-infected animals in comparison with controls was associated with significantly lower numbers of intramural neurons. Other studies have suggested that NO plays a role in the tissue damage seen in Chagas' disease.[21–25] The control of acute-phase *T. cruzi* infection is critically dependent on cytokine-mediated macrophage activation to intracellular killing. Production of interferon (IFN)-γ and tumor necrosis factor-α in *T. cruzi*-infected mice results in the activation of inducible nitric oxide synthase (iNOS) and in elevated NO synthesis, which is critical for trypanocidal activity in macrophages.[22,26–30] In addition, iNOS activation and production of damaging amounts of NO (via generation of more potent oxidants such as peroxynitrite) have been directly implicated in neurodegenerative disorders such as multiple sclerosis and Alzheimer's disease.[31–34]

The present investigation was undertaken to evaluate the direct role that NO plays in the neuronal destruction occurring during acute-phase *T. cruzi* infection in genetically manipulated mice lacking either the iNOS gene or the IFN-γ gene. Intrinsic enteric denervation was observed in *T. cruzi*-infected mice. Our results clearly indicate that this is attributable to the IFN-γ-elicited NO production that results from iNOS activation in the inflammatory foci along the intestinal wall.

Materials and Methods

Animals

Breeding pairs of mice (backcrossed on C57BL/6) with targeted disruption of IFN-γ or iNOS were obtained from Jackson Laboratories (Bar Harbor, ME). The genotypes of these knockout mice (iNOS$^{-/-}$ mice and IFN$^{-/-}$ mice) were determined by using a previously established polymerase chain reaction technique.[35] The knockout mice were bred and maintained, alongside C57BL/6 wild-type (WT) mice, in microisolator cages in the animal facility of the Department of Biochemistry and Immunology, Faculty of Medicine of Ribeirão Preto, University of São Paulo, Ribeirão Preto, Brazil. On reaching the age of 6 to 8 weeks, male animals were selected for study.

Parasites and Experimental Infection

The Y strain of *T. cruzi* was maintained by serial passage from mouse to mouse. Randomly selected WT and knockout mice were infected intraperitoneally with 100 trypomastigote forms of the Y strain of *T. cruzi*. Other randomly selected animals from each of the three groups were injected intraperitoneally with the same volume of saline and served as controls.

Determination of Parasitemia

The course of infection was monitored by periodic analysis of 5-ml blood samples drawn from the tail veins, using a previously described method.[32] Survival rates were determined in parallel groups of animals. Results are expressed as mean ± SEM.

Histopathological Study

On day 10 of infection (coinciding with the day after parasitemia peaked), the animals were sacrificed. The ileum and colon were isolated, each segment was opened along the anti-mesenteric border, and the luminal content was gently removed. The segments were processed according to a standardized protocol.[33] Subsequently, the segments were prefixed in neutral 10% formalin for 90 to 120 minutes, rolled up to form "Swiss rolls," and fixed for an additional 18 to 20 hours. Half of this material was cut into rings, incubated overnight in 15% sucrose, stored at −70°C, and assigned to Hoechst and terminal dUTP nick-end labeling stainings. The other half was processed for paraffin embedding. Serial sections (5 μm thick) were cut from both segments and stained with hematoxylin and eosin, cresyl violet, and immunohistochemistry. Because no change was observed in the histopathological appearance of either segment, the results are presented indistinctly.

Intestinal Parasitism and Inflammation Scores

Tissue parasitism and inflammation scores were estimated in the "Swiss rolls" of colon segments taken from four to five animals from each group. Tissue parasitism scores were determined by counting the total number of amastigote nests, and inflammation scores were determined by counting the number of inflammatory foci, so considered when groups of 10 or more leukocytes were identified. Both counts were performed in a medium-power light microscopic field (×200). For each colon, 35 fields were analyzed.

Neuronal Quantification

Quantification of neurons was performed in the myenteric plexuses of the colon. On days 5 and 10 of infection, annular colonic segments from each of the three groups were fixed in 10% formalin in phosphate-buffered saline (PBS) for 8 hours, dehydrated, and embedded in paraffin. Colonic segments taken from uninfected animals from all three groups were also collected and identified as day 0 of infection. To avoid double counting of the same cell, maximum ganglion cell diameter was morphometrically measured and found to be 25 μm. Serial 5-μm sections, resulting in a total length of 500 μm, were cut. Every fifth section was mounted on a slide and stained with 1% cresyl violet. Therefore, each section actually represented a 25-μm length of tissue, avoiding double counting of neuronal cells. Neurons with lesions that were considered irreversible (no nucleus or nuclear pyknosis) were not scored.

Assessment of Neuronal Damage

Sections (5 μm thick) from ileal and colonic segments were cut on a cryostat and incubated with a Hoesch 33342 fluorescent probe (0.2 μg/ml; Molecular Probes, Eugene, OR). The fluorochrome binds specifically to DNA, and is used to evaluate nuclear appearance, detecting changes such as DNA clumping in apoptotic bodies under appropriate ultraviolet light filtration. In addition, apoptotic nuclei were detected with a TUNEL detection kit (Boehringer Mannheim, Indianapolis, IN) that identifies early fragmentation of the nucleus. Subsequently, sections were hydrated and permeabilized with 0.25% Triton X-100 for 10 minutes, rinsed in PBS, and covered with the labeling reaction mixture containing terminal deoxynucleotidyl transferase and fluorescein-deoxyuridine triphosphate. Sections were incubated at 37°C for 1 hour and the reaction was terminated by rinsing the sections with PBS. The preparations were examined under ultraviolet light through a fluorescein isothiocyanate filter on an Olympus BX51 reflected fluorescence system (Olympus, Tokyo, Japan).

Immunohistochemistry

Sections (5 to 7 μm thick) from ileal and colonic segments were cut on a cryostat and incubated for 30 minutes at 37°C in 1% bovine serum albumin after endogenous peroxidase blocking of nonspecific binding. Primary rabbit anti-iNOS (1:100; Chemicon, Temecula, CA), rabbit anti-PGP 9.5 (1:1000; Ultraclone, UK) antibodies and rabbit anti-*T. cruzi* serum (1:400) were incubated overnight at 4°C. Secondary biotinylated antibodies were goat anti-rabbit antibodies, followed by streptavidin-peroxidase complexes (DAKO-LSAB^R 2 system; DAKO, Carpinteria, CA). The reaction was visualized by incubating the section with 3,3′-diaminobenzidine tetrahydrochloride (Sigma, St. Louis, MO) and counterstaining with hematoxylin. Negative controls were prepared by incubating sections with the preadsorbed antiserum and by replacing primary antiserum with immunoglobulins of the same class and concentration.

Measurement of iNOS Activity

The NO synthase activity was determined by measuring the conversion of L-[U-^{14}C]-arginine to [U-^{14}C]-citrulline.[36] Immediately after collection, the tissues were frozen and stored at −70°C. On the day of assay, the tissues were homogenized at 4°C in homogenizing buffer (pH 7.4; 50 mmol/L Tris, 3.2 mmol/L sucrose, 1 mmol/L dithiothreitol, 10 μg ml^{-1} leupeptin, 10 μg ml^{-1} soybean trypsin inhibitor, 21 μg ml^{-1} aprotinin). The homogenate was centrifuged at 10,000 × *g* for 20 minutes at 4°C and the resultant supernatant, containing both the soluble and particulate NO synthase was added to assay buffer (pH 7.2; 50 mmol/L $KH_2PO_4^-$, 1 mmol/L $MgCL_2$, 0.2 mmol/L $CaCl_2$, 50 mmol/L valine, 20 μmol/L L-citrulline, 20 μmol/L L-arginine, 1 mmol/L dithiothreitol, 100 μmol/L NADPH, 2 μmol/L tetrahydrobiopterin, 3 μmol/L flavin adenine dinucleotide (FAD), 3 μmol/L flavin mononucleotide (FMN), 0.05 μCi~1 μmol/L L-[U-^{14}C]-arginine). After a 30-minute incubation at 37°C, the substrate was removed by adding 1:1 (v/v) Milli-Q water/Dowex-AG-SOW, thereby terminating the reaction. After centrifugation at 5000 × *g* for 10 minutes, the supernatant was carefully removed and NO synthase activity was determined from the conversion of L-[U-^{14}C]-arginine to [U-^{14}C]-citrulline. To determine Ca^{2+}-independent activity, the experiments were performed in the absence of $CaCl_2$ and calmodulin, but in presence of 2 nmol/L of EGTA. The activity of the enzyme was calculated as the difference between the [U-^{14}C]-citrulline generated from control samples and that generated from samples containing the NO synthase inhibitor (L-NMMA, 1 mmol/L). Ca^{2+}-independent NOS-activity was determined as the difference between samples containing EGTA and samples containing EGTA plus L-NMMA. The soluble protein content of the supernatant was determined using the Coomassie blue binding method using a Bio-Rad protein reagent with bovine serum albumin as a standard. The NO synthase activity was expressed as pmol NO min^{-1} mg^{-1} protein.

Statistical Analysis

Data are presented as mean ± SEM of the indicated number of animals or experiments. For statistical analysis, analysis of variance, Tukey test (to correct for multiple comparisons), and Student's *t*-test were used. Values of $P < 0.05$ were considered significant.

Results

Parasitemia and Survival Rate

Compared with infected WT mice, infected iNOS$^{-/-}$ and IFN$^{-/-}$ mice exhibited progressively elevated parasitemia levels after day 8 of infection and until their death (Figure 1A). Knockout mice died between days 8 and 16 of infection with much higher levels of parasitemia than that seen in WT control animals that survived the acute phase of the infection (Figure 1B).

Intestinal Parasitism, Inflammation Scores, and Neuronal Quantification

Mice with disrupted iNOS genes (iNOS$^{-/-}$) that were infected with *T. cruzi* presented higher numbers of amastigote forms of the parasite in the colon (Figure 1C). The number of parasites found in the infected IFN$^{-/-}$ mice was very low (data not shown in Figure 1C). Infected WT mice presented intense inflammatory exudate, not only at the myenteric plexuses, but also at the tunica muscularis and the tela subserosa. The scored inflammation in the tunica muscularis was only slightly more intense in infected WT mice than in infected iNOS$^{-/-}$ mice, although there was no statistically significant difference (Figure 1D).

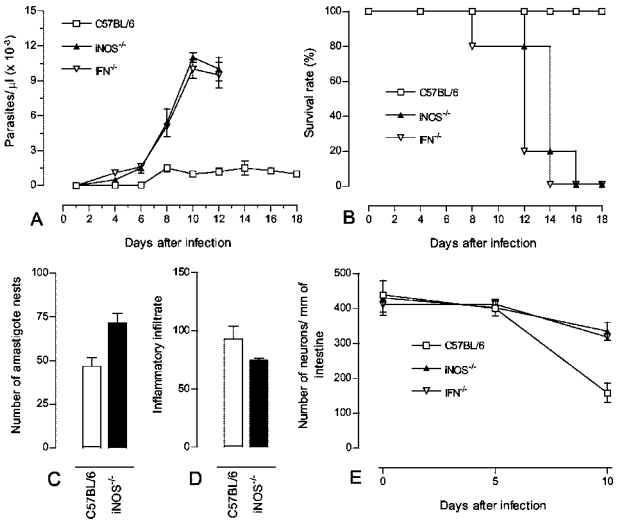

Figure 1. Course of the *T. cruzi* infection-induced neuronal destruction in C57BL/6 WT and in knockout mice (IFN$^{-/-}$ and iNOS$^{-/-}$). Animals were intraperitoneally injected with 100 trypomastigote forms of the Y strain of *T. cruzi*. Parasitemia levels (**A**) and mortality rates (**B**) were evaluated. At 10 days after infection, numbers of amastigote nests (**C**) and inflammatory foci (**D**) in colon segment samples from WT, IFN$^{-/-}$, and iNOS$^{-/-}$ mice were counted in 35 microscopic fields (×200). Data on infected IFN$^{-/-}$ mice are not shown because parasites and inflammatory foci were found in extremely high numbers. Values are expressed as mean ± SEM for 10 mice per group. Data are representative of three independent experiments. The myenteric neuronal number/mm of intestine (**E**) was determined in noninfected and infected mice (5 and 10 days after infection) (each value represents the mean ± SD for at least four animals). Similar results were obtained in three independent experiments. *, $P < 0.05$ comparing infected WT mice with infected IFN$^{-/-}$ and infected iNOS$^{-/-}$ animals.

Practically no inflammatory foci were observed in the colons of infected IFN$^{-/-}$ mice (data not shown in Figure 1D).

The number of myenteric plexus neurons diminished significantly in infected WT animals on day 10 of infection, decreasing by 60% in comparison with noninfected animals. In contrast, neuronal diminution observed in infected IFN$^{-/-}$ and iNOS$^{-/-}$ mice did not reach the level of significance (Figure 1E).

Histopathological Study

On day 10 of infection, all infected WT animals showed some degree of intestinal edema, in the ileum as well as in the colon. Both infected WT mice and infected iNOS$^{-/-}$ mice presented focal changes interposed with normal areas along the intestinal segments studied. Pronounced diffuse inflammatory responses were seen in the tunica muscularis of WT-infected mice. These responses were usually correlated with ruptured parasite nests and included mononuclear cell and neutrophil infiltration, cellular parasitism, and marked diminution and degenerative changes in myenteric plexus ganglion cells (Figure 2A, and inset). The mononuclear cell and neutrophil infiltrate was associated with smooth muscle cell destruction (Figure 2A), ganglion cell degeneration and necrosis (Figure 2C), and apoptosis (Figure 2C, inset). Contrastingly, the changes in infected iNOS$^{-/-}$ mice were characterized by discrete inflammatory foci, mainly composed of mononuclear cells, associated with ruptured parasite nests in the tunica muscularis and tela subserosa. Often, the nests were observed in close proximity with the autonomic ganglia, occasionally in glial cells (Figure 2B), although no inflammatory infiltrate, loss of smooth muscle cells, ganglion cell degeneration, or necrosis was observed (Figure 2, B and D).

iNOS and PGP 9.5 Immunoreactivity

Positive iNOS expression was evident in inflammatory cells near the damaged ganglion cells (Figure 2E) as well as in the smooth muscle cells of the tunica muscularis (Figure 2F) in the intestinal wall of infected WT mice. In contrast, infected iNOS$^{-/-}$ mice presented no detectable iNOS immunoreactivity (Figure 2G), except for weak immunoreactivity in a few parasitized cells (Figure 2H). Decreased numbers of PGP 9.5-positive neurons and fibers were frequently observed in infected WT mice (Figure 3, A and D). The representative aspects of PGP 9.5-staining patterns in infected WT mice decreased in intensity in the ganglia as well as in nerve fiber profiles (Figure 3A) when compared with infected iNOS$^{-/-}$ mice (Figure 3B) or controls (Figure 3C). The myenteric plexuses appeared normal in infected iNOS$^{-/-}$ mice and, despite the presence of parasites and mild inflammatory infiltrate, there was no ganglion cell degeneration (Figure 2B). Marked damage to myenteric ganglia in infected WT mice was associated with loss of PGP 9.5 expression, reflecting neuronal death (Figure 3D). Ganglion cells that had degenerated showed a loss of stainable Nissl substance and displacement of the nuclei to the periphery of the cells (Figure 3E). These degenerative changes were not observed in infected iNOS$^{-/-}$ mice (Figure 3F) or in infected IFN$^{-/-}$ mice (data not shown).

Determination of iNOS Activity

On days 5 and 10 of infection, iNOS activity in infected WT mice was significantly greater than in uninfected controls. In contrast, iNOS activity in infected IFN$^{-/-}$ and iNOS$^{-/-}$ mice remained unchanged after infection with *T. cruzi* (Figure 4).

Discussion

The disturbances in the motility of the gastrointestinal tract, so frequently observed in chronic chagasic patients, are morphologically expressed as hypertrophy of the muscular wall followed by dilatation of the organ.[37] These digestive manifestations of chronic Chagas' disease mainly involve megaesophagus and megacolon, predominantly affecting the sigmoid colon. Significantly lower numbers of myenteric plexus neurons and inflammation are the most evident features of enteromegaly.[3,38] Involvement of the enteric nervous system seems to be an essential element in the pathogenesis of the altered motility and insidious development of the megalic formations.

From systematic investigations of Chagas' disease in humans and in experimentally or naturally infected ani-

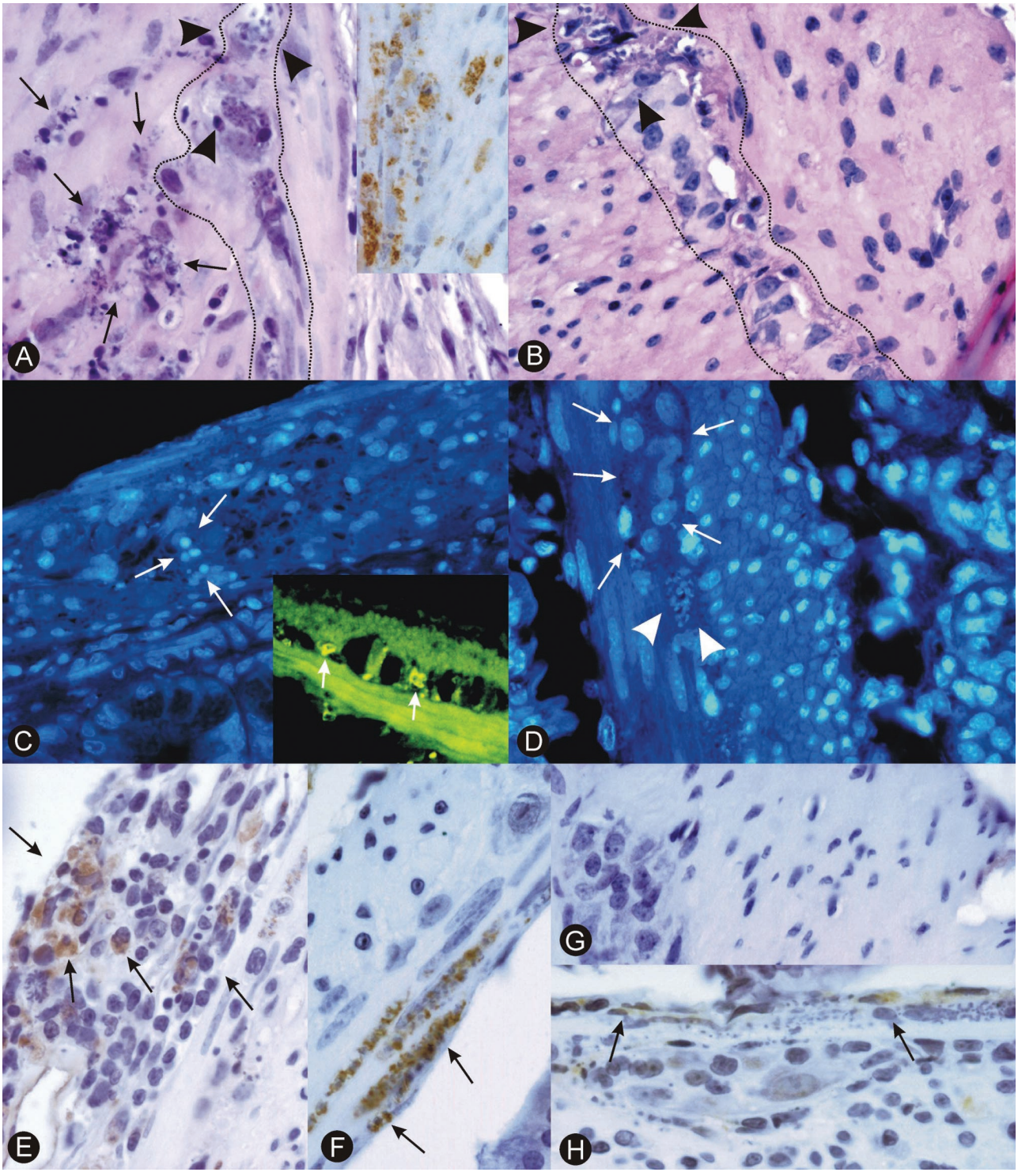

Figure 2. Parasitism, inflammation, and tissue and neuronal damage in intestinal tissue taken from WT and iNOS$^{-/-}$ mice at 10 days after infection with *T. cruzi*. **A:** Intestinal section from WT mouse showing amastigote nests (**arrowheads**) associated with intense inflammatory tissue damage in a myenteric plexus ganglion (delimited by **dotted line**) and in the muscle layer (**arrows**). Notice the borders of the ganglia infiltrated by inflammatory cells that lie very close to damaged neurons. Disrupted parasite nests in the muscle layer are attributable to the striking smooth muscle cell degeneration (H&E). The **inset** in **A** shows *T. cruzi* antigens revealed by immunohistochemistry. **B:** Preserved myenteric plexus ganglion (delimited by a **dotted line**) in an intestinal section from an infected iNOS$^{-/-}$ mouse, showing no significant inflammatory infiltrate or tissue damage. *T. cruzi* amastigote nests can be seen (**arrowheads**) (H&E). Hoechst 33342 fluorescent probe staining of intestinal sections of WT (**C**) and iNOS$^{-/-}$ (**D**) mice for demonstration of apoptotic cells. Neuronal damage is indicated by the characteristic nuclear appearance of DNA clumping in apoptotic bodies (**C**, **arrows**) in a highly damaged myenteric plexus in a WT mouse. The **inset** in **C** shows apoptotic neurons in green by terminal dUTP nick-end labeling labeling of nuclei (**arrows**). Amastigote nest (**arrowheads**) very close to preserved myenteric plexus ganglion cells (**arrows**) is shown in **D**. Immunostaining of iNOS in intestinal sections of infected WT (**E** and **F**) and iNOS$^{-/-}$ (**G** and **H**) mice. Inflammatory (**E**) and parenchymal cells (**F**) of infected WT (**arrows**), but not of infected iNOS$^{-/-}$ mice, are immunoreactive to iNOS, except for a weak immunostaining of a few smooth muscle cells (**H**, **arrows**). Original magnifications: ×400 (**A–H**); ×200 (**insets**).

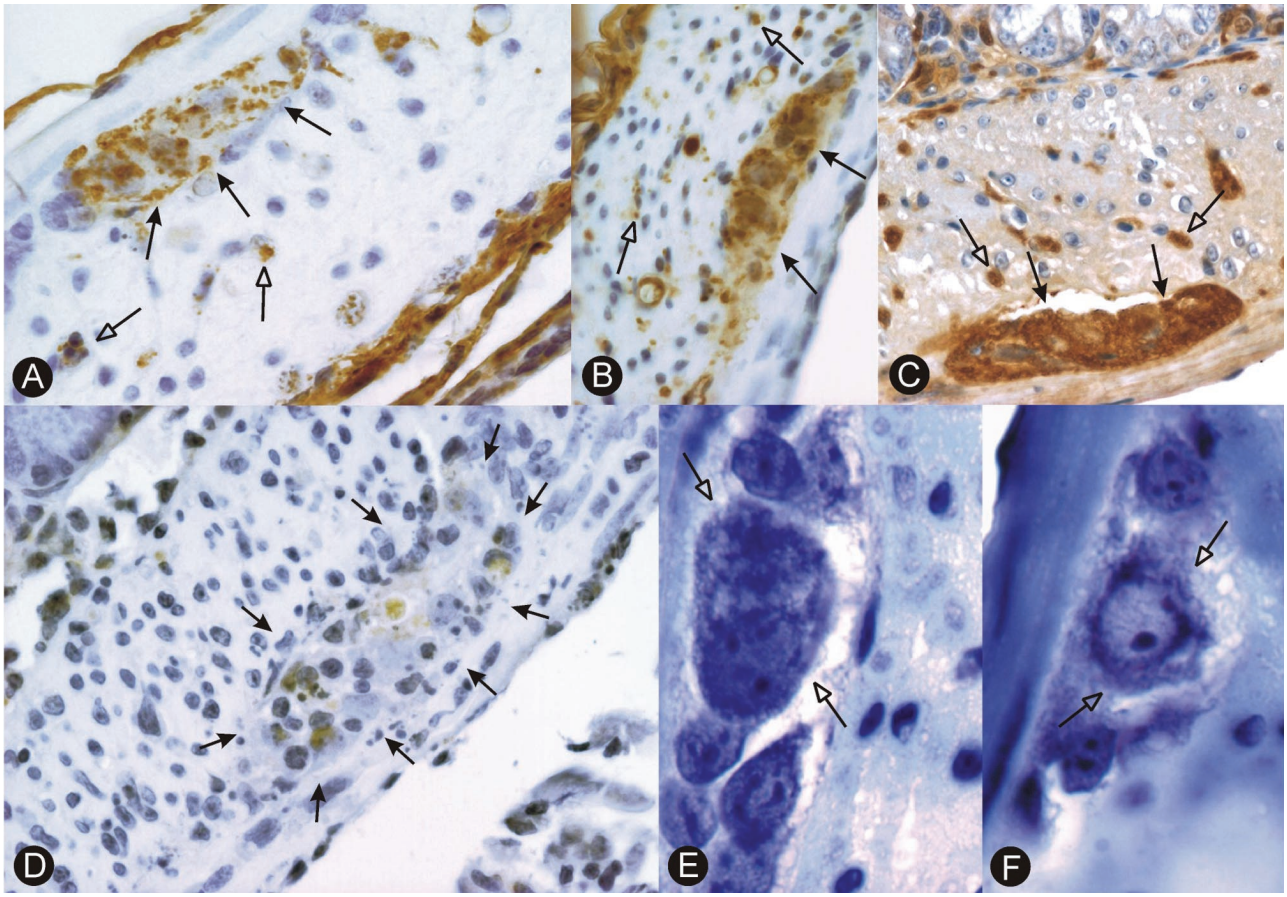

Figure 3. PGP 9.5 immunoreactivity and cresyl violet-staining features of neurons in intestinal sections from infected and noninfected WT mice and from infected iNOS$^{-/-}$ mice. Myenteric ganglia (**arrows**) and transverse profiles of nerves (**open arrows**) in intestinal sections of infected WT (**A** and **D**), infected iNOS$^{-/-}$ (**B**), and noninfected WT (**C**) mice, stained with anti-PGP 9.5 antibody. Notice in **A** and **D** the affected myenteric ganglia in infected WT mice, presenting neuronal loss and lack of PGP 9.5 immunoreactivity. Marked inflammatory reaction can be seen in **D** (delimited by **arrows**). The cresyl violet staining shows neuronal degeneration in infected WT (**E**), but not in infected iNOS$^{-/-}$ (**F**), mice. Notice in **E** the displacement of nuclei to the periphery and the dispersion of the Nissl substance (**open arrows**), in contrast to the normal appearance in (**F**). Original magnifications: ×350 (**A–D**); ×1000 (**E** and **F**).

mals, it has been concluded that nerve cell destruction occurs during the acute phase, and that it occurs in the vicinity of ruptured pseudocysts.[4] Although the mechanism involved in this nerve cell destruction is still undetermined, several hypotheses have been put forth. In light of the fact that ganglion cell lesions appeared after the disintegration of amastigote forms, it has been postulated that a neurotoxic or neurolytic agent is liberated by the disintegration of the amastigote forms.[13] Earlier studies suggested the existence of a toxin to explain certain lesions in the acute phase of the disease.[39] In addition, the observation that, in a restricted area, degeneration and necrosis of multiple cell types follows the disintegration of amastigote forms led to the proposition that a cytotoxin is being liberated.[40,41] Because the existence of a toxin has not been proven, other attempts have been made to explain the nerve cell destruction. Another hypothesis is that direct destruction of nerve cells occurs through parasitism of the nerve cell.[14] However, intensive and thorough studies have shown a very small number of parasitized cells among the hundreds of thousands of ganglion cells in mice, rat, and dogs experimentally infected with *T. cruzi*.[3] Myenteric denervation has also been attributed to the intense inflammatory reaction around the ruptured pseudocysts.[16] Nerve cells, however, are very resistant to specific types of inflammation. This can be seen in two major inflammatory bowel diseases: ulcerative colitis and Crohn's disease, in which there is intense inflammatory infiltrate throughout the intestinal wall, but integrity is preserved in the myenteric and submucosal nerve plexuses.[42] The participation of a immunoallergic mechanism has also been suggested as the cause of nerve cell lesions. Specific autoimmunity against neurons has been demonstrated in chronic Chagas' patients and in mice experimentally infected with *T. cruzi*.[17,19,20] Recently, it was postulated that NO is involved in the peripheral denervation seen in acute-phase experimental *T. cruzi* infection in mice.[21] Compared with controls, infected rats presented significantly reduced neuron counts in the colon and heart resulting from a twofold increase in serum nitrate. Moreover, animals treated with the NO synthase inhibitor *N*-nitro-L-arginine showed marked decreases in serum nitrate concentrations and significant tissular parasitism related to nondiminished numbers of neurons.

Our findings support those from previous studies showing myenteric denervation in acute-phase experimental *T. cruzi* infection. In addition, we clearly demon-

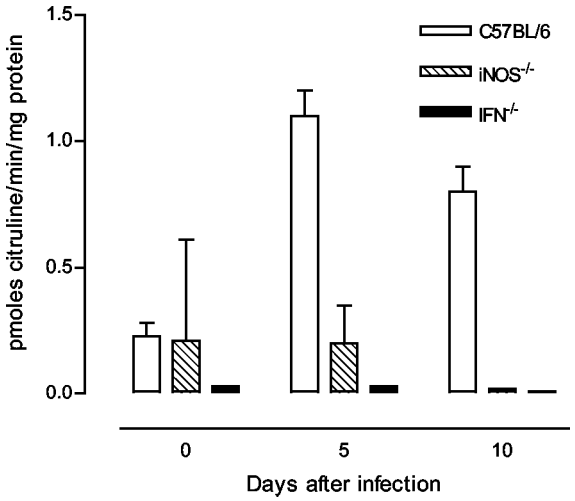

Figure 4. Inducible iNOS activity determined in intestines of *T. cruzi*-infected mice. The iNOS activity was significantly greater in infected WT mice than in infected iNOS$^{-/-}$ or IFN$^{-/-}$ mice. Bars values represent mean ± SEM of pmol/minute/mg of protein measured in three experiments. *, $P < 0.01$; **, $P < 0.001$.

strated that, despite the fact that infected iNOS$^{-/-}$ mice presented greater numbers of parasite nests and similar inflammatory infiltrate in the intestinal wall on day 10 of infection than did infected WT mice, numbers of myenteric plexus neurons were not reduced in the infected iNOS$^{-/-}$ mice. Neuronal nerve profile expression, as revealed by the general nerve marker PGP 9.5, was preserved in the knockout animals. Infected IFN$^{-/-}$ mice did not suffer significant neuronal loss and there was no inflammatory infiltrate in the intestinal wall. These observations suggest that NO could be the final mediator of neuronal damage. The absence of neuronal destruction on day 5 of infection suggests that the intrinsic intestinal denervation could either be secondary to the inflammatory processes, not observed at this time point, or because of the kinetics of NO production.

Production of IFN-γ and tumor necrosis factor-α in *T. cruzi*-infected mice result in the activation of iNOS and in elevated NO synthesis, which is critical for macrophage trypanocidal activity.[26] The microbicidal activity of IFN-γ-treated macrophages against *T. cruzi* involves L-arginine-dependent NO-mediated mechanism, which can be inhibited by interleukin-10 or transforming growth factor-β.[26,43,44] The host/parasite relationship balance manifests, in some instances, as the inflammatory infiltrate intensity *versus* parasite load. Early IFN-γ-dependent activation of iNOS and elevated NO synthesis results in macrophage trypanocidal activity and control of the acute phase of *T. cruzi* infection.[22,26,29,30] In the present study, the higher parasitemia levels and mortality rates of infected IFN$^{-/-}$ and iNOS$^{-/-}$ mice as compared with infected WT mice may reflect defective NO effector functions.[45]

Direct parasitism was not observed in our samples. However, inflammatory foci were commonly seen around parasitized cells near the myenteric neurons in infected WT and iNOS$^{-/-}$ mice. In comparison with infected WT mice, infected iNOS$^{-/-}$ mice presented similar inflammation scores but higher numbers of parasites. In the ganglia of infected iNOS$^{-/-}$ animals, we identified a few parasitized cells as being glial cells (glial fibrillary acidic protein immunoreactivity not shown). In infected WT animals, these cells are not well visualized because the degenerative process affects them as it does the neurons. At present, we cannot rule out the possibility that enteric glial cells play a role as an early source of iNOS-derived NO in our model. This has been described in other degenerative and inflammatory diseases of the central nervous system.[46] Enteric glial cells represent an extensive but relatively poorly described cell population within the gastrointestinal tract. These enteric glial cells represent the morphological and functional equivalent of central nervous system astrocytes within the enteric nervous system. The enteric glial cell network has trophic and protective functions on enteric neurons and is fully implicated in the integration and modulation of neuronal activities.[47] In our model, disruption of the enteric glial cell network may represent one possible cause for the increased neuronal destruction. The absence of inflammatory infiltrate in infected IFN$^{-/-}$ mice is probably related to the complete absence of Mig and IP-10 chemokine expression, as has been previously demonstrated in our laboratory.[27] Infected WT mice presented iNOS immunoreactive inflammatory cells in the vicinity of the myenteric ganglia as well as parasitized cells near the neurons. In contrast, infected iNOS$^{-/-}$ mice presented no detectable iNOS immunoreactivity, except for a weak reaction in a few parasitized cells. In addition, iNOS activity in infected WT mice increased significantly on days 5 and 10 of infection in comparison with uninfected controls. The tissular NO values correspond to the increased levels of $NO2^-$ and $NO3^-$ in the plasma of WT mice in the acute phase of *T. cruzi* infection. As expected, iNOS activity in iNOS$^{-/-}$ and IFN$^{-/-}$ mice did not change after infection with *T. cruzi*.[22] Actually, excessive NO production, often involving iNOS, has been ascribed a role as a major contributor to several disease states.[48]

Despite the complexity and diversity of the role of NO in the inflammatory response,[49] our findings clearly demonstrate that neuronal damage does not occur when the generation of NO is impaired in infected iNOS$^{-/-}$ and IFN$^{-/-}$ mice, regardless of whether inflammatory infiltrate is present (iNOS$^{-/-}$ mice) or absent (IFN$^{-/-}$ mice). In conclusion, our observations strongly indicate that the myenteric denervation seen in the acute phase of *T. cruzi* infection is because of IFN-γ-elicited NO production resulting from iNOS activation of the inflammatory foci along the intestinal wall.

References

1. World Health Organization: Chagas' disease. Tropical Disease Research. Twelfth Program of UNDP/World Bank/WHO Special Program for Research and Training in Tropical Disease Research (TDR). Geneva, World Health Organization, 1993, pp 125–135
2. Rossi MA, Bestetti RB: The challenge of Chagas' cardiomyopathy. The pathologic roles of autonomic abnormalities, autoimmune mechanisms and microvascular changes, and therapeutic implications. Cardiology 1995, 86:1–7

3. Köberle F: Chagas' disease and Chagas' syndromes: the pathology of American trypanosomiasis. Adv Parasitol 1968, 6:63–116
4. Köberle F: The causation and importance of nervous lesions in American trypanosomiasis. Bull WHO 1970, 42:739–743
5. Köberle F: Megaesophagus. Gastroenterology 1958, 34:460–465
6. Köberle F: Megacolon. Trop Med Hyg 1958, 1:21–24
7. Köberle F: Patogenia y anatomia patologica de la enfermedad de Chagas. Bol Ofic Sanit Panamer 1961, 51:404–428
8. Köberle F: Enteromegaly and cardiomegaly in Chagas' disease. Gut 1963, 6:63–116
9. Köberle F: Pathogenesis of Chagas' disease. Ciba Foundation Symposium. Amsterdam, Elsevier-Excerpta Medica-North Holland, 1974, pp 137–158
10. Köberle F, Nador E: Etiologia e patogenia do megaesôfago no Brasil. Rev Paul Med 1955, 47:643–661
11. Köberle F, Alcântara FG: Mecanismo da destruição neuronal do sistema nervoso periférico na Moléstia de Chagas. Hospital 1960, 57:1057–1060
12. Oliveira JSM: A natural human model of intrinsic heart nervous system denervation: Chagas' cardiopathy. Am Heart J 1985, 110:1092–1098
13. Köberle F: Über das neurotoxin des Trypanosoma cruzi. Zbl Allg Path Anat 1956, 95:468–475
14. Okumura M: Contribuição para o estudo das lesões dos neurônios do plexo mientérico do colon na Moléstia de Chagas experimental no camundongo branco (Mus musculus L.). Ph.D. Thesis. Faculty of Medicine, University of São Paulo, 1966
15. Muniz J: Contribuição para um melhor conhecimento da ação patogênica do T. cruzi. Hospital 1967, 72:29–54
16. Tafuri WL: Lesões do sistema nervoso autônomo do coração e do colon do camundongo na fase aguda da doença de Chagas experimental. Estudos ao microscópio ótico e ao eletrônico. Rev Assoc Med Minas Gerais 1968, 19:3–39
17. Ribeiro dos Santos R, Ramos de Oliveira JC, Rossi MA, Köberle F: Antibodies to neurons in chronic Chagas' disease. Trans R Soc Trop Med Hyg 1976, 70:167
18. Khoury EL, Ritacco V, Cossio PN, Languens RP, Szarfman A, Diez C, Araña RM: Circulating antibodies to peripheral nerve in American trypanosomiasis. Clin Exp Immunol 1979, 36:8–12
19. Ribeiro dos Santos R, Márquez JO, Furtado CC, Ramos de Oliveira JC, Martins AR, Köberle F: Antibodies to neurons in chronic Chagas' disease. Tropenmed Parasit 1979, 30:19–23
20. Ribeiro dos Santos R, Hudson L: Trypanosoma cruzi: immunological consequences of parasite modification of host cells. Clin Exp Immunol 1980, 40:36–41
21. Garcia SB, Paula JS, Giovanetti GS, Zenha F, Ramalho EM, Zucoloto S, Silva JS, Cunha FQ: Nitric oxide is involved in the lesions of the peripheral autonomic neurons observed in the acute phase of experimental Trypanosoma cruzi infection. Exp Parasitol 1999, 93:191–197
22. Vespa GN, Cunha FQ, Silva JS: Nitric oxide is involved in control of Trypanosoma cruzi-induced parasitemia and directly kills the parasite in vitro. Infect Immun 1994, 62:5177–5182
23. Ny L, Persson K, Larsson B, Chan J, Weiss LM, Wittner M, Huang H, Tanowitz HB: Localization and activity of nitric oxide synthases in the gastrointestinal tract of Trypanosoma cruzi-infected mice. J Neuroimmunol 1999, 99:27–35
24. Pinto NX, Torres-Hillera MA, Mendoza E, Leon-Sarmiento FE: Immune response, nitric oxide, autonomic dysfunction and stroke: a puzzling linkage on Trypanosoma cruzi infection. Med Hypotheses 2002, 58: 374–377
25. Chandra M, Tanowitz HB, Petkova SB, Huang H, Weiss LM, Wittner M, Factor SM, Shtutin V, Jelicks LA, Chan J, Shirani J: Significance of inducible nitric oxide synthase in acute myocarditis caused by Trypanosoma cruzi (Tulahuen strain). Int J Parasitol 2002, 32:897–905
26. Gazzinelli RT, Oswald IP, Hieny S, James SL, Sher A: The microbicidal activity of interferon-gamma-treated macrophages against Trypanosoma cruzi involves an L-arginine-dependent, nitrogen oxide-mediated mechanism inhibitable by interleukin-10 and transforming growth factor-beta. Eur J Immunol 1992, 22:2501–2506
27. Aliberti JC, Souto JT, Marino AP, Lannes-Vieira J, Teixeira MM, Farber J, Gazzinelli RT, Silva JS: Modulation of chemokine production and inflammatory responses in interferon-gamma- and tumor necrosis factor-R1-deficient mice during Trypanosoma cruzi infection. Am J Pathol 2001, 158:1433–1440
28. Silva JS, Vespa GN, Cardoso MA, Aliberti JC, Cunha FQ: Tumor necrosis factor alpha mediates resistance to Trypanosoma cruzi infection in mice by inducing nitric oxide production in infected gamma interferon-activated macrophages. Infect Immun 1995, 63:4862–4867
29. Machado FS, Martins GA, Aliberti JC, Mestriner FL, Cunha FQ, Silva JS: Trypanosoma cruzi-infected cardiomyocytes produce chemokines and cytokines that trigger potent nitric oxide-dependent trypanocidal activity. Circulation 2000, 102:3003–3008
30. Saeftel M, Fleischer B, Hoerauf A: Stage-dependent role of nitric oxide in control of Trypanosoma cruzi infection. Infect Immun 2001, 69:2252–2259
31. Beckman JS, Beckman TW, Chen J, Marshall PA, Freeman BA: Apparent hydroxyl radical production by peroxynitrite: implications for endothelial injury from nitric oxide and superoxide. Proc Natl Acad Sci USA 1990, 87:1620–1624
32. Bo L, Dawson TM, Wesselingh S, Mork S, Choi S, Kong PA, Hanley D, Trapp BD: Induction of nitric oxide synthase in demyelinating regions of multiple sclerosis brains. Ann Neurol 1994, 36:778–786
33. Lee SC, Zhao ML, Hirano A, Dickson DW: Inducible nitric oxide synthase immunoreactivity in the Alzheimer disease hippocampus: association with Hirano bodies, neurofibrillary tangles, and senile plaques. J Neuropathol Exp Neurol 1999, 58:1163–1169
34. Smith MA, Richey Harris PL, Sayre LM, Beckman JS, Perry G: Widespread peroxynitrite-mediated damage in Alzheimer's disease. J Neurosci 1997, 17:2653–2657
35. Pfeffer K, Matsuyama T, Kündig TM, Wakeham M, Mak TW: Mice deficient for 55kd tumor necrosis factor receptor are resistant to endotoxic shock, yet succumb to L monocytogenes infection. Cell 1993, 73:457–467
36. Rees DD, Cunha FQ, Assreuy J, Herman AG, Moncada S: Sequential induction of nitric oxide synthase by Corynebacterium parvum in different organs of the mouse. Br J Pharmacol 1995, 114:689–693
37. Oliveira RB, Troncon LEA, Dantas RO, Meneghelli UG: Gastrointestinal manifestations of Chagas' disease. Am J Gastroenterol 1998, 93:884–889
38. Tafuri WL: Light and electron microscope studies of the autonomic nervous system in experimental and human American Trypanosomiasis. Virchows Arch 1971, 354:136–149
39. Torres CBM: Sôbre a anatomia patológica da doença de Chagas. Mem Inst Oswaldo Cruz 1941, 36:391–4041
40. Alvarenga RJ: Lesões do tecido adiposo na fase aguda da doença de Chagas experimental, em camundongos (Inaugural Dissertation). Minas Gerais, University of Minas Gerais School of Medicine, 1960
41. MacClure E, Poche R: Die experimentelle Chagas-Myokarditis bei der weiβen Maus im elektonenmikroskopischen Bild. Virchows Arch 1960, 333:405–420
42. Neunlist M, Aubert P, Toquet C, Oreshkova T, Barouk J, Lehur PA, Schemann M, Galmiche JP: Changes in chemical coding of myenteric neurones in ulcerative colitis. Gut 2003, 52:84–90
43. Silva JS, Twardzik DR, Reed SG: Regulation of Trypanosoma cruzi infection in vitro and in vivo by transforming growth factor-beta. J Exp Med 1991, 174:539–545
44. Silva JS, Morrissey P, Grabstein KH, Mohler K, Anderson D, Reed SR: IL-10 and IFN-gamma regulation of experimental Trypanosoma cruzi infection. J Exp Med 1992, 175:169–174
45. Holscher C, Kohler G, Muller U, Mossmann H, Schaub GA, Brombacher F: Defective nitric oxide effector functions lead to extreme susceptibility of Trypanosoma cruzi-infected mice deficient in gamma interferon receptor or inducible nitric oxide synthase. Infect Immun 1998, 66:1208–1225
46. Brown GC, Bal-Price A: Inflammatory neurodegeneration mediated by nitric oxide, glutamate, and mitochondria. Mol Neurobiol 2003, 27:325–355
47. Cabarrocas J, Savidge TC, Liblau RS: Role of enteric glial cells in inflammatory bowel disease. Glia 2003, 41:81–93
48. Drew B, Leeuwenburgh C: Aging and the role of reactive nitrogen species. Ann NY Acad Sci 2002, 959:66–81
49. Gwee KA, Graham JC, McKendrick MW, Collins SM, Marshall JS, Walters SJ, Read NW: Psychometric scores and persistence of irritable bowel after infectious diarrhea. Lancet 1996, 347:150–153